Published in final edited form as:
Brain Res. 2010 November 29; 1362: 23–31. doi:10.1016/j.brainres.2010.09.027.

Characterization of sensory neurons in the dorsal root ganglia of *Bax*-deficient mice

Hiromichi Suzuki[a,1], **Youhei Aoyama**[a,1], **Kouji Senzaki**[a], **Michelle Vincler**[b], **Shannon Wittenauer**[b], **Masaaki Yoshikawa**[a,c], **Shigeru Ozaki**[a,*], **Ronald W. Oppenheim**[c], and **Takashi Shiga**[a]

[a]Graduate School of Comprehensive Human Sciences, University of Tsukuba, Tsukuba, Ibaraki, Japan

[b]Department of Anesthesiology, Wake Forest University School of Medicine, Winston-Salem, NC, USA

[c]Department of Neurobiology and Anatomy and Neuroscience Program, Wake Forest University School of Medicine, Winston-Salem, NC, USA

Abstract

During development, the rescue of spinal motoneurons as well as sensory neurons in the dorsal root ganglion (DRG) from programmed cell death (PCD) depends on the integrity of peripheral target innervation. Following deletion of the pro-apoptotic gene *Bax*, both motoneurons and DRG neurons are rescued from PCD. In the present paper, we asked whether different cell types in the DRG exhibit distinct responses to *Bax* deletion. In 1 month-old *Bax*-deficient (*Bax*−/−) mice, distinct subsets of DRG neurons that were immunopositive for TrkA, CGRP, TRPV1 or TrkC, were all increased in number and exhibited cell atrophy compared to wild type DRG neurons. In addition there was hyperinnervation of the epidermis by CGRP immunopositive processes and a correlated functional hypersensitivity of mechanical nociception in *Bax*−/− mice. By contrast, the functional properties of populations of rescued thermoreceptor and mechanoreceptor DRG neurons were unchanged. These data indicate that although *Bax* deletion rescues all of the DRG cell types examined here from PCD, the functional consequences of having excess cells differ between sensory phenotypes.

Keywords

programmed cell death; *Bax*; dorsal root ganglion; peripheral innervation; neurotrophic factor

1. Introduction

Programmed cell death (PCD) occurs widely during ontogeny and is an important process in the normal development and maintenance of body tissues. In the nervous system, more than half of the neurons produced following neurogenesis are eliminated by PCD (Oppenheim et

[*]**Corresponding author** Graduate School of Comprehensive Human Sciences, University of Tsukuba, 1-1-1 Tennoudai, Tsukuba, Ibaraki 305-8574, Japan Phone: +29-853-2972, Fax: +29-853-2972, ozakis@md.tsukuba.ac.jp .
[1]These authors contributed equally to this work.

al., 1991). With regard to the PCD observed in motoneurons and sensory neurons in the dorsal root ganglion (DRG), limiting amounts of trophic factors derived from peripheral targets are thought to be crucial for promoting and maintaining survival of these neurons (the “neurotrophic hypothesis”) (Hamburger and Levi-Montalcini, 1949; Oppenheim, 1991; Oppenheim and von Bartheld, 2008).

Neurons undergoing developmental PCD typically exhibit characteristics of apoptosis. Proteins of the Bcl-2 family are known to be regulators of apoptosis within the nervous system (Oppenheim and von Bartheld, 2008) and Bax, a pro-apoptotic member of that family, is critically involved in the PCD of most developing neurons including motoneurons and DRG neurons (Buss et al., 2006a, b; Kinugasa et al., 2002; Kinugasa et al., 2006; Sun et al., 2003; White et al., 1998). In *Bax*-deficient (*Bax*−/−) mice, many of the excess motoneurons rescued from PCD exhibit smaller-sized soma, unmyelinated axons and fail to innervate muscle targets (Buss et al., 2006a, b; Kinugasa et al., 2002; Sun et al., 2003). However, the differentiation of rescued DRG neurons in *Bax*−/− mice is less clear, although they also appear to differ from wild type cells. The DRG is composed of subpopulations of sensory neurons which innervate skins, muscles, joints, blood vessels and viscera (Hunt et al., 1992; Lawson, 1992). Two of the major subpopulations of sensory DRG neurons are cutaneous neurons, which convey information from thermoreceptors, nociceptors and mechanoceptors in the skin, and proprioceptive cells, which convey information from muscle spindles regarding muscle length and from Golgi tendon organs regarding muscle tension. These subpopulations of DRG neurons exhibit different molecular characteristics, have specific peripheral and central targets, and require different target-derived trophic factors for their survival, differentiation and maintenance (Ernsberger, 2009; Kirstein and Farinas, 2002; Oppenheim and von Bartheld, 2008). For example, large-sized proprioceptive DRG neurons express TrkC, a receptor for neurotrophin-3 (NT-3), whereas some small-sized nociceptive DRG neurons express TrkC, a receptor for nerve growth factor (NGF), as well as calcitonin gene-related peptide (CGRP); and other small- and medium-sized DRG neurons respond to non-noxious heat and chemical stimuli and express TRPV1, a receptor for capsaicin.

In an attempt to gain further insight into the role of PCD in the nervous system, we have characterized the differentiation and function of distinct subsets of DRG neurons of young adult *Bax*−/− mice.

2. Results

2.1. Effect of *Bax* deletion on the number of DRG neurons

Several previous studies have reported that the number of DRG neurons in *Bax*−/− mice is markedly increased compared with that of *Bax*+/+ mice (Kinugasa et al., 2006; Sun et al., 2003). These results indicate that *Bax* deficiency rescues DRG neurons from PCD. However, it is unclear whether there are quantitative or qualitative differences among the different DRG subtypes in *Bax*−/− mice.

We first examined the number of DRG neuron subtypes at P28 using selective marker antibodies against TrkA, CGRP and TRPV1. Many TrkA- immunopositive ($TrkA^+$) and CGRP- immunopositive ($CGRP^+$) neurons convey nociceptive information, while TRPV1-immunopositive ($TRPV1^+$) neurons respond to heat and chemical stimuli. Figure 1A and E show $TrkA^+$ neurons in the fourth lumbar (L4) DRG of each genotype. In both genotypes, the cytoplasm, but not nuclei, was densely stained. TrkA expression was detected in small and medium-sized DRG neurons. The total number of $TrkA^+$ DRG neurons was 2,135 ± 312 and 3,265 ± 338 (mean ± SEM) in *Bax*+/+ (n = 4) and *Bax*−/− (n = 4) mice, respectively ($p < 0.05$). CGRP expression in the L4DRG is shown in Fig. 1B and F. Similar to TrkA

expression, $CGRP^+$ labeling was detected in the cytoplasm of small and medium-sized DRG neurons of both genotypes. The total number of $CGRP^+$ DRG neurons was 1,483 ± 179 and 2,606 ± 228 in *Bax*+/+ (n = 3) and *Bax*−/− (n = 3) mice, respectively ($p < 0.05$). $TRPV1^+$ labeling was also detected in the cytoplasm of L4DRG neurons (Fig. 1 C, G). The total number of $TRPV1^+$ DRG neurons was 1,859 ± 40 and 2,848 ± 341 in *Bax*+/+ (n = 3) and *Bax*−/− (n = 3) mice, respectively ($p < 0.05$).

Next, we examined the number of proprioceptive DRG neurons using a selective marker antibody against TrkC. Photomicrographs in Fig. 1 D and H show TrkC-immunopositive ($TrkC^+$) neurons in the L3DRG of each genotype. The total number of $TrkC^+$ DRG neurons was 728 ± 92 and 1,254 ± 185 in *Bax*+/+ (n = 4) and *Bax*−/− (n = 4) mice, respectively ($p < 0.05$).

In summary, these findings demonstrate that various subsets of DRG neurons examined here in *Bax*−/− mice are increased by 1.5-1.8 times compared to *Bax*+/+ mice, indicating that supernumerary DRG neurons of several different sensory subclasses are rescued from developmental PCD and are maintained in *Bax*−/− mice up to P28.

2.2. The effect of *Bax* deletion on the size of DRG neurons

Because myelinated dorsal root axons of *Bax*−/− neonates are reported to have a reduced diameter compared to controls (Kinugasa et al., 2006), it seems likely that DRG soma size may also be reduced. In order to examine this possibility, the cross-sectional area of subsets of DRG neurons was analyzed.

Figure 2 shows size-frequency histograms plotted for cross-sectional area of the soma of DRG neurons expressing each marker molecule in both genotypes. The average size of $TrkA^+$ DRG neurons was 267.9 ± 3.2 μm^2 (n = 2,820 cells from 4 DRGs), vs 254.5 ± 2.6 μm^2 (n = 4,387 cells from 4 DRGs), in *Bax*+/+ and *Bax*−/− mice, respectively (Fig. 2 A). In both genotypes, about 70% of $TrkA^+$ DRG neurons were less than 300 μm^2 in cross-sectional area. However, $TrkA^+$ DRG neurons in *Bax*−/− mice were significantly smaller than those in *Bax*+/+ mice ($p < 0.0001$). The distribution of CGRP+ DRG neuron soma size is shown in Fig. 2B. The average size of $CGRP^+$ DRG neurons was 216.5 ± 3.7 μm^2 (n = 1,464 cells from 3 DRGs), vs 205.4 ± 2.5 μm^2 (n = 2,589 cells from 3 DRGs), in *Bax*+/+ and *Bax*−/− mice, respectively. Over 80% of $CGRP^+$ DRG neurons in both genotypes were small (< 300 μm^2), and there was not a significant difference in $CGRP^+$ DRG neuron size between *Bax*+/+ and *Bax*−/− mice ($p = 0.10$). As shown in Fig. 2C, about 80% of $TRPV1^+$ DRG neurons were also small (< 300 μm^2). The average size of $TRPV1^+$ DRG neurons was 232.8 ± 3.2 μm^2 (n = 1,868 cells from 3 DRGs), vs 222.6 ± 2.5 μm^2 (n = 2,828 cells from 3 DRGs), in *Bax*+/+ and *Bax*−/− mice, respectively ($p < 0.001$). In *Bax*+/+ mice, about 90% of $TrkC^+$ DRG neurons were medium to large-sized (≥300 μm^2) (Fig. 2D) and about 40% of $TrkC^+$ DRG neurons were larger than 600 μm^2. The average size of $TrkC^+$ DRG neurons in *Bax*+/+ mice was 579.6 ± 8.1 μm^2 (n = 970 cells from 4 DRGs). In contrast, in *Bax*−/− mice, about 40% of $TrkC^+$ DRG neurons were small (< 300 μm^2) and only about 15% of $TrkC^+$ DRG neurons were larger than 600 μm^2. The average size of $TrkC^+$ DRG neurons in *Bax*−/− mice was 389.4 ± 4.9 μm^2 (n = 1,672 cells from 4 DRGs), a statistically significant difference versus *Bax*+/+ mice ($p < 0.0001$). Taken together, these findings indicate that supernumerary DRG neurons for different sensory modalities are atrophic, raising the possibility that *Bax* deficiency may result in abnormal sensory reception and behavior.

2.3. Cutaneous projections of subsets of DRG neurons in *Bax*−/− mice

In order to examine whether supernumerary cutaneous DRG neurons observed in *Bax*−/− mice innervate their peripheral targets, we visualized the projection of subsets of cutaneous DRG neurons in the hind limb paw.

Sensory innervation of the epidermis of the hind paw skin was analyzed by immunostaining against protein gene product 9.5 (PGP 9.5), a pan-neuronal marker, and CGRP. Both $PGP9.5^+$ afferents and $CGRP^+$ afferents were observed in the epidermis of both genotypes (Fig. 3) and some $PGP9.5^+$ afferents also co-expressed CGRP (arrowheads in Fig. 3) and these processes appear to be thinner than afferents expressing PGP9.5 alone. The total length of all the fragments of $PGP9.5^+$ and $CGRP^+$ fibers in the region of interest is defined as the cumulative length. The density and the cumulative length of both $PGP9.5^+$ fibers and $CGRP^+$ fibers per unit area (1,000 μm^2) are summarized in Table 1. Both the density and the cumulative length of the $CGRP^+$ fibers were significantly increased in *Bax*−/− mice. The ratio of $CGRP^+$ afferents to $PGP9.5^+$ afferents (cumulative length) was also significantly higher in *Bax*−/− mice vs *Bax*+/+ mice. These data suggest that supernumerary $CGRP^+$ DRG neurons in *Bax*−/− mice contribute to hyperinnervation by noxious afferents in the epidermis.

$TRPV1^+$ afferents were detected in the epidermis of the hind paw skin in both genotypes (Fig. 4). The average density of $TRPV1^+$ afferent in the epidermis per unit area (1,000 μm^2) was calculated. There was no significant difference between *Bax*+/+ n = 4) and *Bax*−/− n = 4) mice, 0.099 ± 0.009 and 0.105 ± 0.002, respectively, suggesting that supernumerary $TRPV1^+$ DRG neurons do not result in the excess projection of thermoceptive afferents to the *Bax*−/− hind paw skin.

Non-noxious mechanoceptive afferents of Meissner's corpuscles were identified as $PGP9.5^+$ oval-shaped nerve terminals which lie in the tips of the dermal papillae of the hind paw skin. As shown in Fig. 5, $PGP9.5^+$ oval-shaped nerve terminals frequently occupied the dermal papillae in *Bax*+/+ and *Bax*−/− mice. The number of dermal papillae was 6.8 ± 1.1 (*Bax*+/+) and 5.6 ± 1.3 (*Bax*−/−) and the number of Meissner's corpuscles was 4.7 ± 0.8 (*Bax*+/+) and 3.3 ± 1.0 (*Bax*−/−). The ratio of Meissner's corpuscle-containing dermal papillae was 62.6 ± 5.0% and 56.8 ± 4.2%, in the foot pad of *Bax*+/+ (n = 4) vs *Bax*−/− (n = 3) mice, respectively. The lack of differences in these parameters between genotypes suggests that supernumerary afferents to Meissner's corpuscles does not occur in *Bax*−/− mice.

2.4. Behavioral analysis of sensory function in *Bax*−/− mice

In order to examine whether *Bax*−/− mice exhibit abnormal function in specific sensory modalities, behavioral tests were employed in 1 month-old mice. We first measured mechanical nociceptive thresholds in each genotype and the average pressure required to elicit tail withdrawal is shown in Table 2. The average reaction pressure of 1 month-old mice was 63.7 ± 1.6 s vs 47.1 ± 3.3 s, in *Bax*+/+ (n= 7) and *Bax*−/− (n = 7) mice, respectively ($p < 0.01$).

We next estimated thermoreceptive responses in *Bax*−/− mice by means of heat radiation focused on the plantar surface of the hind paw (Table 2). The average reaction latency did not differ between genotypes: 4.6 ± 0.2 s vs 4.8 ± 0.2 s, in *Bax*+/+ (n = 7) and *Bax*−/− (n = 7) mice, respectively. We also examined mechanical sensitivity to non-noxious stimuli using von Frey filaments applied to the plantar surface of the hind paw. The average number of paw withdrawals in response to both filaments (0.7 g and 1.2 g) was comparable in the two groups (Table 2). These behavioral results are consistent with the increased projection of $CGRP^+$ afferents to the *Bax*−/− hind paw skin.

3. Discussion

We have characterized the properties of different subtypes of DRG neurons rescued from PCD by *Bax* deletion. Using selective marker antibodies against TrkA, CGRP, TRPV1 and TrkC, we observed in P28 *Bax*−/− mice that neurons of each DRG subtype were increased in number and that each subtype (except the $CGRP^+$ cells) exhibit decreased soma size. However, the $CGRP^+$ neurons mediating mechanical nociception but not $TRPV1^+$ neurons exhibit hyperinnervation of peripheral targets and altered sensory responses in *Bax*−/− mice.

3.1. Survival of subsets of DRG neurons in *Bax*−/− mice

Previous studies have reported that apoptosis is undetectable in DRG neurons of *Bax*−/− embryos, indicating a complete rescue of DRG neurons from developmental PCD (Sun et al., 2003; White et al., 1998). Consequently, there are greatly increased numbers of DRG neurons in *Bax*−/− vs *Bax*+/+ mice at embryonic stages (Sun et al., 2003; White et al., 1998). In newborn and adult *Bax*−/− mice, there are also 1.5 times more myelinated DRG axons in dorsal roots (Buss et al., 2006a; Kinugasa et al., 2006; Sun et al., 2003) indicating that DRG neurons rescued from PCD are maintained postnatally although they seem to be smaller-sized and atrophic. We have examined additional characteristics of major subsets of DRG neurons conveying nociceptive, thermoreceptive and proprioceptive information in P28 *Bax*−/− mice using specific molecular markers, and find that $TrkA^+$, $CGRP^+$, $TRPV1^+$ and $TrkC^+$ DRG neurons are all markedly increased in number (1.5-1.8 times), compared to *Bax*+/+ mice. These data indicate that all subpopulations of DRG neurons are rescued from PCD by *Bax* deletion and are maintained until at least P28.

3.2. Atrophy and peripheral projections of DRG neurons in *Bax*−/− mice

Both DRG neurons and spinal motoneurons saved from PCD in *Bax*−/− mice have been shown to be small-sized and atrophic (Buss et al., 2006a; Kinugasa et al., 2002; Kinugasa et al., 2006; Sun et al., 2003). In the present study, the soma size of $TrkA^+$, $TRPV1^+$ and $TrkC^+$ DRG neurons (but not $CGRP^+$ cells) of *Bax*−/− mice is significantly smaller than in *Bax*+/+ mice. Neonatal sympathetic neurons from *Bax*−/− mice exhibit soma atrophy in the absence of NGF, a TrkA ligand, and soma hypertrophy in the presence of NGF (Deckwerth et al., 1996). NGF-dependent and NT-3 dependent DRG neurons are also reduced in size in *Bax*−/−/*NGF*−/− and *Bax*−/−/*NT-3*−/− neonates (Patel et al., 2000; Patel et al., 2003). Loss of target innervation following sciatic nerve axotomy induced soma atrophy (but not cell death) in lumbar DRG neurons of *Bax*−/− neonates (Kinugasa et al., 2006) consistent with a role for target-derived signals in the growth and maintenance of cell size in the DRG. Taken together, these results are consistent with observations of spinal motoneurons in *Bax*−/− mice (Sun et al., 2003). In that study, it was proposed that excess motoneurons rescued from PCD by *Bax* deletion compete for limiting amounts of trophic support from muscle targets, that the winners grow and differentiate normally, and maintain synaptic contact with the target, whereas the losers fail to sustain contact with targets which results in loss of innervation and atrophy. Excess sensory neurons in the *Bax*−/− DRG, may also lose innervation of peripheral targets and exhibit atrophy. Indeed, in the present study we observe that the soma size of $TrkC^+$ DRG neurons was greatly reduced (67%) in *Bax*−/− mice. Proprioceptive as well as some cutaneous mechanoceptive neurons are known to be dependent on NT-3 and its receptor TrkC (Ernsberger, 2009; Kirstein and Farinas, 2002; Oppenheim and von Bartheld, 2008). Adult *Bax*−/− mice exhibit increased numbers of muscle spindles and normal motor behavior on tests of balance and coordination (Buss et al., 2006a). We have shown that P28 *Bax*−/− mice also exhibit normal mechanical sensitivity to non-noxious stimuli. Although these findings suggest that, despite increased cell numbers, proprioceptive and/or mechanoreceptive function is normal in *Bax*−/− mice, further analysis of the stretch reflex pathway is needed to assess proprioceptive function in *Bax*−/− mice.

Despite the marked excess of cutaneous DRG neurons in *Bax*−/− mice, there was only a minor (5%) decrease in soma size of $TrkA^+$, $CGRP^+$ and $TRPV1^+$ DRG neurons. Accordingly, the regulation of soma size of cutaneous DRG neurons vs proprioceptive $TrkC^+$ neurons (and motoneurons) in *Bax*−/− mice may be regulated differently. For example, there was no significant soma atrophy in $CGRP^+$ DRG neurons of *Bax*−/− mice, despite a marked (180%) increase in $CGRP^+$ neurons. CGRP+ fibers in the epidermis of the hind limb paw were increased in *Bax*−/− mice, consistent with the possibility that all or most surviving $CGRP^+$ DRG neurons attain sufficient trophic support from peripheral targets to maintain innervation and the behavioral evidence for hypersensitivity of mechanical nociception indicates that the excess innervation is functional.

These data suggest that DRG neurons in *Bax*−/− mice are represented by at least two subtype populations that differ regarding their response to rescue from PCD. One involves highly competitive, point-to-point connections (as occurs between motoneurons and skeletal muscle targets) and is characteristic of excess rescued proprioceptive sensory neurons and muscle spindle targets where the losers become denervated and atrophy. The other subtype is represented by cutaneous sensory neurons in which the excess rescued neurons innervate their targets and obtain sufficient trophic support resulting in functional hypersensitivity as observed here for $CGRP^+$ DRG neurons.

The difference between these two population may reflect the ability of the cutaneous sensory neurons to regulate the production of target-derived trophic support in an innervation-dependent manner such that in the face of excess neurons and hyperinnervation (*Bax*−/−) there is increased production of target-derived trophic factor (Harper and Davies, 1990). A testable prediction from this hypothesis is that the expression of NGF is increased in the peripheral targets of cutaneous DRG neurons of *Bax*−/− mice, whereas NT-3 is unchanged in the peripheral targets of *Bax*−/− proprioceptive DRG neurons.

4. Experimental procedures

4.1. Animals

Bax-mutant mice (Knudson et al., 1995) were purchased from the Jackson Laboratory (USA) and maintained on a C57BL/6J background. *Bax*+/+ and *Bax*−/− mice were obtained from the overnight mating of the heterozygotes (*Bax*+/−).

Mouse genotyping was performed by PCR using a set of three primers: *Bax* exon 5 forward primer (5′-TGATCAGAACCATCATG-3′), *Bax* intron 5 reverse primer (5′–GTTGACCAGAGTGGCGTAGG-3′), and Neo reverse primer (5′–CCGCTTCCATTGCTCAGCGG-3′). Cycling parameters were 5 min at 94 °C for one cycle plus 30 cycles of 1 min at 94 °C, 1 min at 55 °C, and 1 min at 72 °C. PCR products were resolved on 2% agarose gels.

All the experiments followed the Guide for the Care and Use of Laboratory Animals described by the National Institutes of Health (USA), and were approved by the Animal Experimentation Committee of the University of Tsukuba and the Animal Care and Use Committee of the Wake Forest University Medical Center.

4.2. Immunohistochemistry for DRG neurons

At P28, mice were deeply anesthetized and perfused transcardially with 4% paraformaldehyde (PFA) in 0.1 M phosphate buffer (pH 7.4) (PB).

The L3 and L4 DRG on either the left or right side were isolatated and processed as described below. In each genotype (*Bax*+/+ and *Bax*−/−), a total of 8 DRGs from 4 animals

were used for immunohistochemistry. For cryostat sections, specimens were postfixed in the same fixative for 48 hours at 4°C and immersed in graded concentrations (10%, 20%, 30%) of sucrose solution in 0.1M PB at 4°C. After freezing in Tissue Tek O.C.T. compound (Sakura Finetek), 10 μm thick sections of the DRG were cut serially and every third section was collected onto separate MAS-coated glass slides (Matsunami Glass Ind.). Sections were air-dried for 1 hour and subjected to heat induced epitope retrieval by heating to 105°C for 3 minutes in Dako REAL™ Target Retrieval Solution (Dako). After treatment for 30 minutes at room temperature (RT) with 0.3% H_2O_2 in methanol, the sections were incubated for 1 hour at RT in a blocking solution containing 1% bovine serum albumin and 0.1% Triton X-100 in 0.1M PB. For immunohistochemical analysis, the following antibodies were used: rabbit anti-TrkA antibody (a gift from Dr. F. Reichardt; 1:16,000), rabbit anti-CGRP antibody (Chemicon; 1:4,000), rabbit anti-TRPV1 antibody (Calbiochem; 1:2,000) and goat anti-TrkC antibody (R&D systems; 1:2,000).

The sections were incubated overnight at 4°C with each of the primary antibodies in the blocking solution. The sections were incubated with a biotinylated secondary antibody (Vector Laboratories; 1:500) for 1 hour at RT and processed with the Elite ABC kit (Vector Laboratories) for 30 minutes at RT. Positive reactions were visualized with 3, 3′-diaminobenzidine (DAB) using the ImmunoPure metal enhanced DAB substrate kit (Pierce). Both *Bax*+/+ and *Bax*−/− littermates were processed simultaneously for immunohistochemistry.

4.3. Quantification of DRG neurons

For counts of immunopositive DRG neurons, every third serial section from the DRG was photographed at 20× on an AxioVision photomicroscope (Carl Zeiss). The number of immunopositive DRG neurons was determined by counting neurons that contained a nucleus and showed strong signal intensity in the cytoplasm, as described previously (Nakamura et al., 2008). The total number of immunopositive neurons was calculated from segment matched DRGs of each genotype (14-30 sections were measured in each DRG). Immunopositive DRG neurons were also traced to measure the soma cross-sectional area by using AxioVision Rel. 4.6 (Carl Zeiss).

4.4. Immunohistochemistry for peripheral innervations

The hind paw on either the left or right side was removed from each genotype (*Bax*+/+, n = 4; *Bax*−/−, n = 3) at P28 for immunohistochemistry of PGP9.5 and CGRP. Under deep anesthesia, mice were perfused transcardially with 4% PFA in 0.1 M PB. The hind paw skin was dissected, postfixed with the same fixative and frozen as described above. Sagittal cryostat sections were made at 14 μm thickness and were collected onto MAS-coated glass slides and air-dried for 1 hour. The sections were incubated for 1 hour at RT in the blocking solution as described above. For immunohistochemical analysis, the following antibodies were used: rabbit anti-PGP 9.5 antibody (Chemicon; 1:1,000), and goat anti-CGRP antibody (UltraClone Limited; 1:500). The sections were incubated for 48 hours at 4°C with combination of the primary antibodies in the blocking solution, followed by Alexa Fluor 594-labeled donkey anti-rabbit IgG antibody and Alexa Fluor 488-labeled donkey anti-goat IgG antibody (Invitrogen; 1:1000). To determine the precise location of Alexa Fluor 594-labeled fibers in the skin, the sections were counterstained fluorescently by 0.0001% acridine orange (Wako Chemical).

For anti-TRPV1 immunostaining, the right hind paw skin was dissected from deeply anesthetized P28 mice (*Bax*+/+, n = 4; *Bax*−/−, n = 4), and the skin was fresh-frozen without fixation. Sagittal cryostat sections at 20 μm thickness were collected onto MAS-coated glass slides and fixed in 4% PFA and 0.2% picric acid in 0.1 M PB for 10 minutes. Using the

same procedure described above, the sections were incubated with rabbit anti-TRPV1 antibody (Chemicon; 1:1,500) for 48 hours at 4°C and visualized using Alexa Fluor 594-labeled goat anti-rabbit IgG antibody (Invitrogen; 1:1,000).

Both *Bax*+/+ and *Bax*−/− littermates were processed simultaneously and the sections were photomicrographed at 20× with an adequate fluorescence filter set, and collected as digital images. Immunolabeled profiles in the glabrous footpad (6-27 digital images in each sample) were traced by a tablet (Wacom) and analyzed by using the NIH ImageJ program.

4.5. Behavioral tests

One month-old mice were examined in behavioral tests (*Bax*+/+, n = 7; *Bax*−/−, n = 7). Mechanical sensitivity to non-noxious stimuli was measured by applying 0.7 g and 1.2 g von Frey Filaments (Stoelting) to the plantar surface of mouse hind paws as described previously (Colburn et al., 1999). Mice were placed in individual plexiglass chambers on an elevated mesh surface and the number of paw withdrawals in three sets of 10 applications (total = 30) for each filament was used to determine mechanical sensitivity for each group of mice. Mechanical nociceptive thresholds were measured using an Analgesy-Meter (Ugo-Basile). Mice were held gently and a constant rate of increasing pressure (16 g/sec) was applied to the mouse tail. The pressure required to elicit tail withdrawal was determined once (1 trial), and a maximum pressure of 250 g was used to avoid tissue damage. Thermoreceptive thresholds were evaluated using a commercially available paw thermal stimulator (Anesthesiology Research Laboratory) as described previously (Hargreaves et al., 1988). Mice were placed in plexiglass chambers on a glass floor maintained at 30°C for 30 minutes. A radiant heat light source 48-50°C was focused on the plantar surface of either hind paw and the time for foot withdrawal was recorded. Both paws were tested once in a random order and the mean paw withdrawal latency was calculated. A 30 second cut-off was employed to avoid tissue damage.

4.6. Statistical analysis

All results are expressed as the mean ± SEM. The Mann-Whitney *U*-test and the Student's *t*-test were employed for statistical analysis of morphological and behavioral data, respectively. Differences were considered significant if the probability of error was less than 5%.

RESEARCH HIGHLIGHTS

- *Bax* deletion rescued all subtypes of DRG neurons from programmed cell death.
- The excess DRG neurons exhibited decreased soma size following *Bax* deletion.
- The only CGRP positive neurons showed skin hyperinnervation in *Bax*-deficient mice.
- The functional consequences of having excess DRG neurons differ between subtypes.

Acknowledgments

This work was supported by NIH grants, NS048982 and NS53527 (R.W.O.) and NS048158 (M.V.), USA and by a Grant-in-Aid 21300130 from the JSPS, Japan (T.S.) and by the Organization for the Support and Development of Strategic Initiatives, University of Tsukuba, Japan (S.O., T.S.)

Abbreviations

dorsal root ganglion	DRG
programmed cell death	PCD
neurotrophin-3	NT-3
nerve growth factor	NGF
calcitonin gene-related peptide	CGRP
protein gene product 9.5	PGP 9.5

References

Buss RR, Gould TW, Ma J, Vinsant S, Prevette D, Winseck A, Toops KA, Hammarback JA, Smith TL, Oppenheim RW. Neuromuscular development in the absence of programmed cell death: phenotypic alteration of motoneurons and muscle. J. Neurosci. 2006a; 26:13413–13427. [PubMed: 17192424]

Buss RR, Sun W, Oppenheim RW. Adaptive roles of programmed cell death during nervous system development. Annu. Rev. Neurosci. 2006b; 29:1–35. [PubMed: 16776578]

Colburn RW, Rickman AJ, DeLeo JA. The effect of site and type of nerve injury on spinal glial activation and neuropathic pain behavior. Exp. Neurol. 1999; 157:289–304. [PubMed: 10364441]

Deckwerth TL, Elliott JL, Knudson CM, Johnson EM Jr. Snider WD, Korsmeyer SJ. BAX is required for neuronal death after trophic factor deprivation and during development. Neuron. 1996; 17:401–411. [PubMed: 8816704]

Ernsberger U. Role of neurotrophin signalling in the differentiation of neurons from dorsal root ganglia and sympathetic ganglia. Cell Tissue. Res. 2009; 336:349–384. [PubMed: 19387688]

Hamburger V, Levi-Montalcini R. Proliferation, differentiation and degeneration in the spinal ganglia of the chick embryo under normal and experimental conditions. J. Exp. Zool. 1949; 111:457–501. [PubMed: 18142378]

Hargreaves K, Dubner R, Brown F, Flores C, Joris J. A new and sensitive method for measuring thermal nociception in cutaneous hyperalgesia. Pain. 1988; 32:77–88. [PubMed: 3340425]

Harper S, Davies AM. NGF mRNA expression in developing cutaneous epithelium related to innervations density. Development. 1990; 110:515–519. [PubMed: 2133552]

Hunt, SP.; Mantyh, PW.; Priestley, JV. The organization of biochemically characterized sensory neurons. In: Scott, SA., editor. Sensory neurons. Diversity, development, and plasticity. Oxford University Press; New York: 1992. p. 60-76.

Kinugasa T, Ozaki S, Hamanaka S, Kudo N. The effects of sciatic nerve axotomy on spinal motoneurons in neonatal Bax-deficient mice. Neurosci. Res. 2002; 44:439–446. [PubMed: 12445631]

Kinugasa T, Kudo N, Ozaki S. Peripheral targets influence sensory-motor connectivity in the neonatal spinal cord: sciatic nerve axotomy in Bax-deficient mice. Neurosci. Res. 2006; 54:30–37. [PubMed: 16290239]

Kirstein M, Farinas I. Sensing life: regulation of sensory neuron survival by neurotrophins. Cell. Mol. Life Sci. 2002; 59:1787–1802. [PubMed: 12530514]

Knudson CM, Tung KS, Tourtellotte WG, Brown GA, Korsmeyer SJ. Bax-deficient mice with lymphoid hyperplasia and male germ cell death. Science. 1995; 270:96–99. [PubMed: 7569956]

Lawson, SN. Morphological and biochemical cell types of sensory neurons. In: Scott, SA., editor. Sensory neurons. Diversity, development, and plasticity. Oxford University Press; New York: 1992. p. 27-59.

Nakamura S, Senzaki K, Yoshikawa M, Nishimura M, Inoue K, Ito Y, Ozaki S, Shiga T. Dynamic regulation of the expression of neurotrophin receptors by Runx3. Development. 2008; 135:1703–1711. [PubMed: 18385258]

Oppenheim RW. Cell death during development of the nervous system. Annu. Rev. Neurosci. 1991; 14:453–501. [PubMed: 2031577]

Oppenheim RW, Prevette D, Yin QW, Collins F, MacDonald J. Control of embryonic motoneuron survival in vivo by ciliary neurotrophic factor. Science. 1991; 251:1616–1618. [PubMed: 2011743]

Oppenheim, RW.; von Bartheld, C. Neurotrophins and programmed cell death. In: Squire, LR., editor. Fundamental Neuroscience. Academic Press; San Diego: 2008. p. 437-468.

Patel TD, Jackman A, Rice FL, Kucera J, Snider WD. Development of sensory neurons in the absence of NGF/TrkA signaling in vivo. Neuron. 2000; 25:345–357. [PubMed: 10719890]

Patel TD, Kramer I, Kucera J, Niederkofler V, Jessell TM, Arber S, Snider WD. Peripheral NT3 signaling is required for ETS protein expression and central patterning of proprioceptive sensory afferents. Neuron. 2003; 38:403–416. [PubMed: 12741988]

Sun W, Gould TW, Vinsant S, Prevette D, Oppenheim RW. Neuromuscular development after the prevention of naturally occurring neuronal death by Bax deletion. J. Neurosci. 2003; 23:7298–7310. [PubMed: 12917363]

White FA, Keller-Peck CR, Knudson CM, Korsmeyer SJ, Snider WD. Widespread elimination of naturally occurring neuronal death in Bax-deficient mice. J. Neurosci. 1998; 18:1428–1439. [PubMed: 9454852]

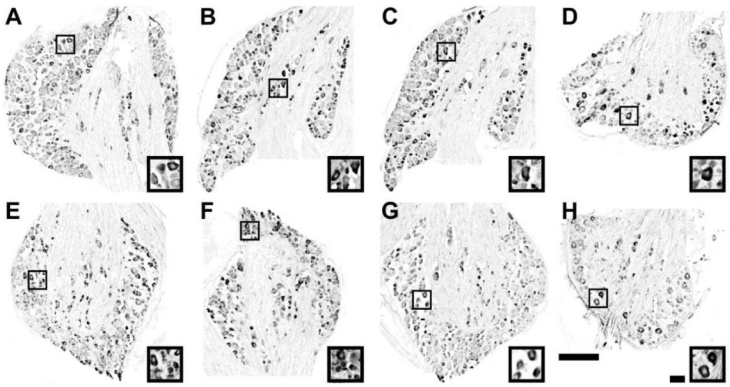

Figure 1.

Immunoreactivity of TrkA (A, E), CGRP (B, F), TRPV1 (C, G), and TrkC (D, H), in the DRG of *Bax*+/+ (A-D) and *Bax*−/− (E-H) mice at P28.

Boxed areas in each low power view are enlarged in the insets. Scale bars: 200 μm for lower power and 40 μm for higher power images.

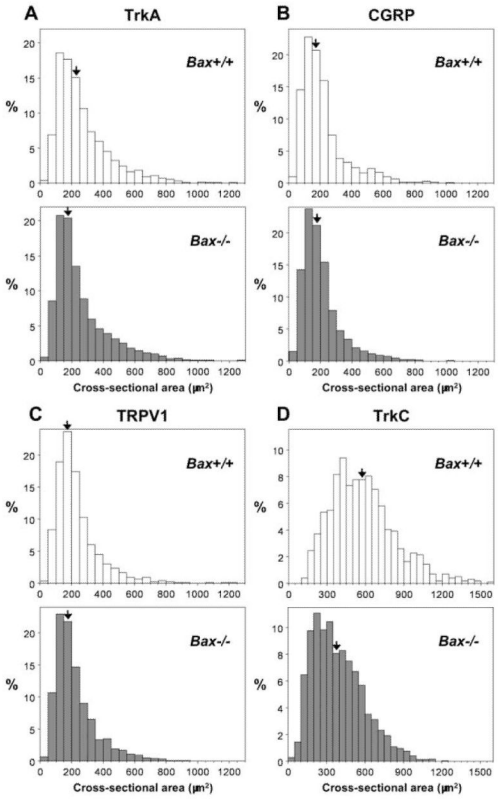

Figure 2.

Soma size distribution of subsets of DRG neurons in *Bax*+/+ and *Bax*−/− mice at P28. Size frequency (percent, ordinate) histograms were plotted from cross-sectional areas (abscissa) of DRG neurons expressing TrkA (A), CGRP (B), TRPV1 (C) and TrkC (D) on the abscissa. Open and solid columns represent *Bax*+/+ and *Bax*−/− mice, respectively. Each arrow indicates the column with the median values.

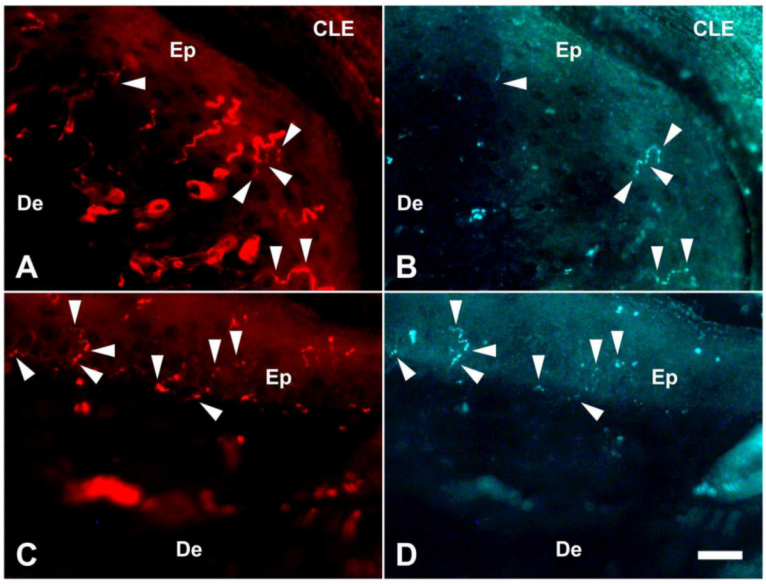

Figure 3.

Sensory fibers innervating the epidermis in the hind limb paw of *Bax*+/+ and *Bax*−/− mice at P28. PGP9.5^{+} fibers (A, C) and CGRP^{+} fibers (B, D) photographed in the same microscopic field. Photos from *Bax*+/+ and *Bax*−/− mice are shown in A, B and C, D, respectively. Arrowheads indicate sensory fibers co-expressing PGP9.5 and CGRP. CLE: corneal layer of epidermis, De: dermis, Ep: epidermis. Scale bar: 20 μm.

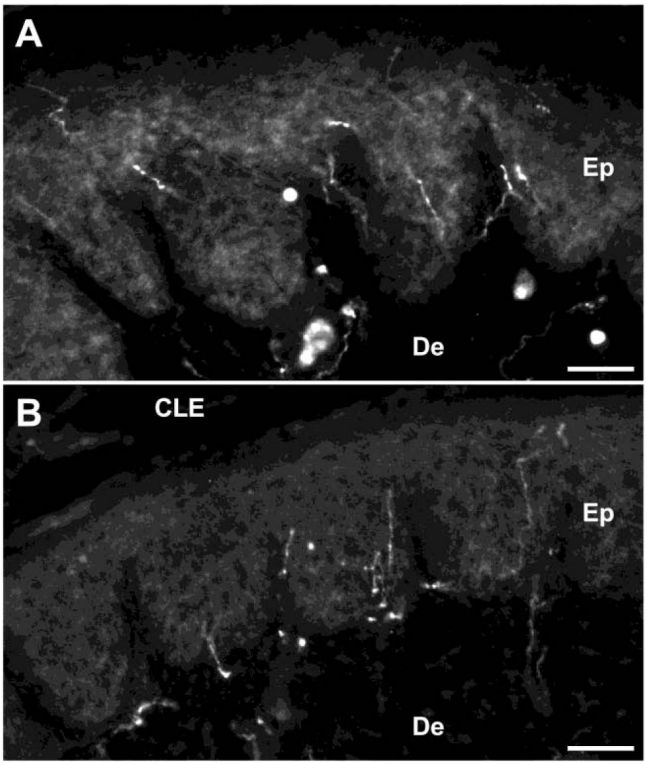

Figure 4.
TRPV1^{+} afferent projections to the hind paw skin of *Bax*+/+ (A) and *Bax*−/− (B) mice at P28. CLE: corneal layer of epidermis, De: dermis, Ep: epidermis. Scale bars: 50 μm.

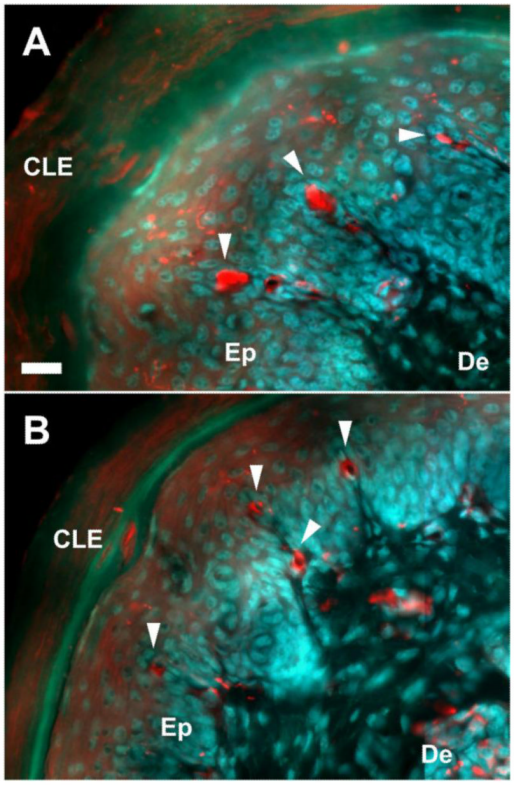

Figure 5.

Sensory fibers innervating the hind limb paw of *Bax*+/+ and *Bax*−/− mice at P28. Merged image of photomicrographs of PGP9.5^{+} sensory fibers (red) and counterstaining with acridine orange (blue) in the foot pad of *Bax*+/+ (A) and *Bax*−/− (B) mice. Meissner corpuscles are identified as PGP9.5^{+} oval-shaped nerve terminals (arrowheads) which lie in the dermal papillae. CLE: corneal layer of epidermis, De: dermis, Ep: epidermis. Scale bar: 20 μm.

Table 1

Peripheral sensory projections to the hind paw skin of *Bax*+/+ and *Bax*−/− mice at P28.

	***Bax*+/+**	***Bax*−/−**
Density of PGP9.5$^+$ fibers (per 1,000 μm^2)	0.85 ± 0.11 n = 4	1.11 ± 0.19 n = 3
Cumulative length of PGP9.5$^+$ fibers (μm) (per 1,000 μm^2)	5.60 ± 1.01 n = 4	4.91 ± 0.64 n = 3
Density of CGRP$^+$ fibers (per 1,000 μm^2)	0.04 ± 0.01 n = 4	0.11 ± 0.02* n = 3
Cumulative length of CGRP$^+$ fibers (μm) (per 1,000 μm^2)	0.29 ± 0.07 n = 4	0.67 ± 0.06* n = 3
% of cumulative length of CGRP$^+$ to PGP9.5$^+$ fibers (per 1,000 μm^2)	5.4 ± 1.4 n = 4	13.8 ± 0.8* n = 3

Mean ± SEM, n indicates the number of animals examined.

*; $p < 0.05$, significantly different from *Bax*+/+ by Mann-Whitney *U*-test.

Table 2

Behavioral tests examined in 1 month-old *Bax*+/+ and *Bax*−/− mice.

Test	Condition	*Bax*+/+	*Bax*−/−
Mechanical nociception (Analgesy-meter)	Pressure increasing rate 16 g/s	Reaction pressure (g) 63.7 ± 1.6 n = 7	47.1 ± 3.3* n = 7
Thermoreception (Heat radiation)	Radiant heat source 48-50°C	Reaction latency (s) 4.6 ± 0.2 n = 7	4.8 ± 0.2 n = 7
Non-noxious mechanoception (von Frey)	Filament pressure	No. of reactions	
	0.7 g	7.3 ± 0.8 n = 7	9.3 ± 1.1 n = 7
	1.2 g	13.0 ± 0.9 n = 7	14.6 ± 1.3 n = 7

Mean ± SEM, n indicates the number of animals examined.

*; $p < 0.01$, significantly different from *Bax*+/+ by Student's *t*-test